Columbia International Publishing
Journal of Modeling, Simulation, Identification, and Control
(2014) Vol. 2. No. 1 pp. 18-30
doi:10.7726/jmsic.2014.1002
Research Article

Galloping of Wind-excited Tower under External Excitation and Parametric Damping

Lahcen Mokni, Ilham Kirrou, Mohamed Belhaq *

Received 31 March 2014; Published online 14 June 2014

Abstract

This paper investigates the influence of combined fast external excitation and parametric damping on the amplitude and the onset of galloping of a tower submitted to steady and unsteady wind flow. A lumped single degree of freedom model is considered and the cases where the turbulent wind activates either external excitation, parametric one or both are studied. The methods of direct partition of motion and the multiple scales are used to drive the slow flow near primary resonance. The influence of the combined excitation on the galloping is examined. The results shown that not only the amplitude of galloping is influenced, but also the onset of galloping.

Keywords: Periodic galloping; Parametric damper; Fast excitation; Wind effect; Structural dynamics; Perturbation analysis; Control

1. Introduction

The control of large amplitude oscillations in tall flexible building constitutes an important issue in the design and stability of such structures. Considerable efforts have been made to reduce the amplitude of oscillations of tall building induced by steady and unsteady wind. It is well known that above a certain threshold of the wind speed, tall buildings develop galloping (Parkinson and Smith, 1964; Novak, 1969; Nayfeh and Abdel-Rohman, 1990a; Abdel-Rohman, 2001b; Clark and Modern, 2004) causing the structure to oscillate with large amplitudes. In this context, considerable efforts have been done to quench such wind-induced oscillations including, for instance, mass tuned dampers, tuned liquid dampers, internal parametric damping or external excitation. A review of some control methods and their full-scale implementation to civil infrastructure applications is given in Spencer and Nagarajaiah (2003).

The effect of unsteady wind on the galloping onset of towers has been considered by several authors. In (Abdel-Rohman, 2001b) a single degree of freedom (sdof) model has been considered and the multiple scales method (MSM) Nayfeh and Balachandran (1995) has been used to analyze the influence of the unsteady wind on the critical wind speed above which galloping occurs. It was shown that the unsteady wind decreases significantly

*Corresponding email: mbelhaq@yahoo.fr
Laboratory of Mechanics, University Hassan II-Casablanca, Morocco

the galloping onset only near the primary resonance. In (Luongo and Zulli, 2011a; Zulli and Luongo, 2012b), the effect of parametric, external and self-induced excitation on periodic galloping of a single tower and of two towers linked by a nonlinear viscous device was examined. Recently, the effect of fast harmonic excitation (FHE) on periodic and quasiperiodic galloping onset of a tower exposed to steady and unsteady wind was studied near primary resonance (Belhaq et al, 2013a). The introduction of a FHE as a control strategy was motivated by an experimental work made for vibrating testing purpose of a full size tower (Keightley et al, 1961). The mechanical vibration exciter system used in such an experiment is placed on the top of the structure and debits a harmonic excitation to the structure. More recently, the influence of internal parametric damping (IPD) on periodic galloping onset of a tower under steady and unsteady wind was examined (Mokni et al, 2014). It was concluded that when the unsteady wind is present, IPD decreases the amplitude of galloping in all cases of loading, but has no influence on the galloping onset. The IPD can be introduced via a damper device in the interfloors damping as reported in (Munteanu et al, 2013). Its use as a control strategy was motivated by its simple implementation and beneficial effect in reducing vibration in many engineering applications.

In this paper, we extend the results given in (Belhaq et al, 2013a; Mokni et al, 2014) by focusing on the combined effect of FHE and IPD on periodic galloping. The main purpose is to examine how FHE and IPD can influence the galloping of the wind-excited tower when they are introduced simultaneously.

The paper is organized as follows: In Section 2, the equation of motion including the effect of both external excitation and parametric damping is given. The method of DPM (Blekhman, 2000; Thomsen, 2003) is performed and the MSM is applied in section 3 to derive the modulation equations of the slow dynamic near the primary resonance. In Section 4, we analyze the combined effect of FHE and IPD on the periodic galloping in the cases where the unsteady wind activates different excitations. Section 5 concludes the work.

2. Equation of Motion and Slow Flow

A single mode approach of the tower motion is considered and a sdof lumped mass model is introduced (Abdel-Rohman, 2001b; Luongo and Zulli, 2011a). It is assumed that the tower is subjected to steady and unsteady wind and to a combined effect of FHE and IPD. In this case, the dimensionless sdof equation of motion can be written in the form

$$\ddot{x} + x + \big[c_a(1-\bar{U}) - b_1 u(t)\big]\dot{x} + Y\nu^2\cos(\nu t)\dot{x} + b_2\dot{x}^2 + \big[\frac{b_{31}}{\bar{U}} + \frac{b_{32}}{\bar{U}^2}u(t)\big]\dot{x}^3 = \eta_1\bar{U}u(t) + \eta_2\bar{U}^2 + Y\cos(\nu t) \quad (1)$$

where the dot denotes differentiation with respect to the non-dimensional time t. Equation (1) contains, in addition to the elastic, viscous and inertial linear terms, quadratic and cubic components in the velocity generated by the aerodynamic forces. The steady component of the wind velocity is represented by $\bar{U}$ and the turbulent wind flow is approximated by a periodic force, $u(t)$, which is assumed to include the two first harmonics, $u(t) = u_1\sin\Omega t + u_2\sin 2\Omega t$, where u_1, u_2 and Ω are, respectively, the amplitudes and the fundamental frequency of the response. We shall analyze the case of external excitation, $u(t) = u_1\sin\Omega t$, parametric one, $u(t) = u_2\sin 2\Omega t$, and the case where external and parametric excitations are present simultaneously. The coefficients of Eq. (1) are given in Appendix I and we assume that Y, ν are, respectively, the dimensionless amplitude and the frequency of the FHE and IPD as well. To simplify the analysis, we consider the particular case where the FHE and the IPD have the same amplitude Y and the same frequency ν.

Equation (1) includes a slow dynamic due to the steady and unsteady wind and a fast dynamic induced by the FHE and the IPD. To separate these dynamics, we perform the method of DPM on Eq. (1) by defining a fast time $T_0 = \nu t$ and a slow time $T_1 = t$, and splitting up $x(t)$ into a slow part $z(T_1)$ and a fast part $\phi(T_0, T_1)$ as

$$x(t) = z(T_1) + \mu\phi(T_0, T_1) \quad (2)$$

where z describes the slow main motions at time-scale of oscillations, $\mu\phi$ stands for an overlay of the fast motions and μ indicates that $\mu\phi$ is small compared to z. Since ν is considered as a large parameter, we choose $\mu \equiv \nu^{-1}$ for convenience. The fast part $\mu\phi$ and its derivatives are assumed to be $2\pi-$periodic functions of fast time T_0 with zero mean value with respect to this time, so that $< x(t) >= z(T_1)$ where $<>\equiv \frac{1}{2\pi}\int_0^{2\pi}() \, dT_0$ defines time-averaging operator over one period of the fast excitation with the slow time T_1 fixed. Averaging procedure gives the following equation governing the slow dynamic of motion

$$\ddot{z} + z + \big[c_a(1-\bar{U}) - b_1 u(t) - H_0 + \big(\frac{b_{31}}{\bar{U}} + \frac{b_{32}}{\bar{U}^2}u(t)\big)H_1\big]\dot{z} + \big[B - B_0\big(\frac{b_{31}}{\bar{U}} + \frac{b_{32}}{\bar{U}^2}u(t)\big)\big]\dot{z}^2 + \big[\frac{b_{31}}{\bar{U}} + \frac{b_{32}}{\bar{U}^2}u(t)\big]H_2\dot{z}^3 = \eta_1\bar{U}u(t) + \eta_2\bar{U}^2 + G \tag{3}$$

where $H_0 = 4b_2Y^2$, $H_1 = 6(\frac{Y}{\nu})^2$, $H_2 = 1 + 6Y^2\nu^2$, $B = b_2(1 + 2Y^2\nu^2)$, $B_0 = 12Y^2$ and $G = -2b_2(\frac{Y}{\nu})^2$. Note that the case without FHE has been studied in Belhaq et al, (2013a), the case without IPD was considered in Mokni et al, (2014), while the case without FHE and IPD ($Y = 0$) was talked in Luongo and Zulli, (2011a).

To obtain the modulation equations of the slow dynamic (3) near primary resonance, the MSM is performed by introducing a bookkeeping parameter ε, scaling as $z = \varepsilon^{\frac{1}{2}}z$, $b_1 = \varepsilon b_1$, $H_0 = \varepsilon H_0$, $H_1 = \varepsilon H_1$, $B = \varepsilon^{\frac{1}{2}}B$, $B_0 = \varepsilon^{\frac{1}{2}}B_0$, $\eta_1 = \varepsilon^{\frac{3}{2}}\eta_1$, $\eta_2 = \varepsilon^{\frac{3}{2}}\eta_2$ and assuming that $\bar{U} = 1 + \varepsilon V$ (Luongo and Zulli, 2011a), with the resonance condition $\Omega = 1 + \varepsilon\sigma$ where V stands for the mean wind velocity and σ is a detuning parameter, a two-scale expansion of the solution is sought in the form

$$z(t) = z_0(t_0, t_1) + \varepsilon z_1(t_0, t_1) + O(\varepsilon^2) \tag{4}$$

where $t_i = \varepsilon^i t$ $(i = 0, 1)$. In terms of the variables t_i, the time derivatives become $\frac{d}{dt} = d_0 + \varepsilon d_1 + O(\varepsilon^2)$ and $\frac{d^2}{dt^2} = d_0^2 + 2\varepsilon d_0 d_1 + O(\varepsilon^2)$, where $d_i^j = \frac{\partial^j}{\partial^j t_i}$. Substituting Eq. (4) into Eq. (3), equating coefficients of the same power of ϵ, we obtain the two first orders of approximation

$$d_0^2 z_0 + z_0 = G \tag{5}$$

$$\begin{aligned} d_0^2 z_1 + z_1 = -2d_0 d_1 z_0 + (c_a V + b_1 u(t_0) + H_0 - H_1(b_{31} + b_{32}u(t_0)))(d_0 z_0) \\ -(B - B_0(b_{31} + b_{32}u(t_0)))(d_0 z_0)^2 - H_2(b_{31} + b_{32}u(t_0))(d_0 z_0)^3 + \eta_1 u(t_0) + \eta_2 \end{aligned} \tag{6}$$

A solution of Eq. (5) is given by

$$z_0 = A(t_1)\exp(it_0) + \bar{A}(t_1)\exp(-it_0) + G \tag{7}$$

where i is the imaginary unit and A is an unknown complex amplitude. Equation (6) can be solved for the complex amplitude A by introducing its polar form as $A = \frac{1}{2}ae^{i\phi}$. Substituting the expression of A into Eq. (7) and eliminating the secular terms, the modulation equations of the amplitude a and the phase ϕ can be extracted as

$$\begin{cases} \dot{a} = [S_1 - S_3\sin(2\phi)]a - S_5\cos(\phi)a^2 + [-S_2 + 2S_4\sin(2\phi)]a^3 - \beta\cos(\phi) \\ a\dot{\phi} = [\sigma - S_3\cos(2\phi)]a + 3S_5\sin(\phi)a^2 + [S_4\cos(2\phi)]a^3 + \beta\sin(\phi) \end{cases} \tag{8}$$

where $S_1 = \frac{1}{2}(c_a V + H_0 - H_1 b_{31})$, $S_2 = \frac{3}{8}b_{31}H_2$, $S_3 = \frac{1}{4}(b_1 - H_1 b_{32})u_2$, $S_4 = \frac{1}{8}b_{32}H_2 u_2$, $S_5 = \frac{1}{8}b_{32}B_0 u_1$ and $\beta = \frac{\eta_1 u_1}{2}$. It can be seen that the FHE and the IPD influence the dynamic of the tower via the coefficients $H_i (i = 0, 1, 2)$ and B_0.

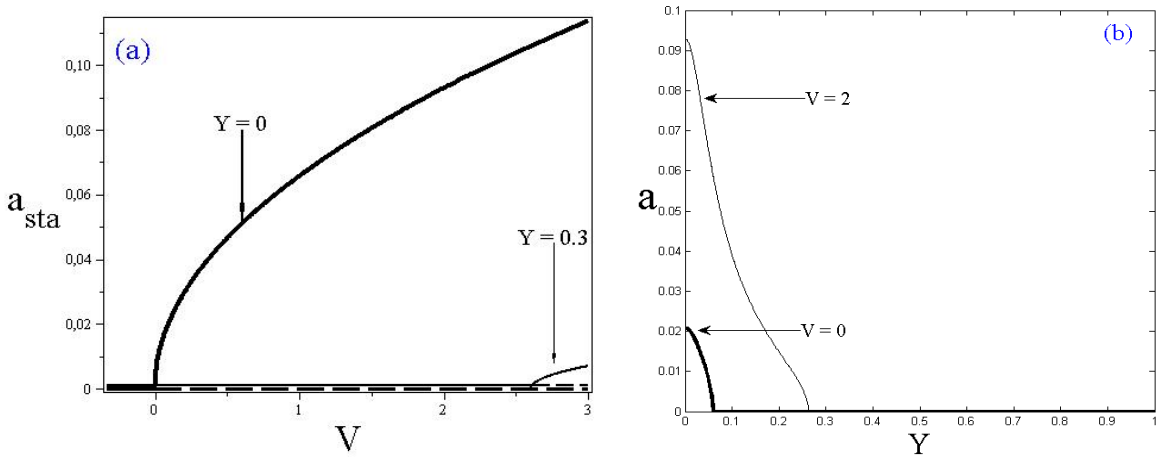

Figure 1. (a) Equilibrium branches, (b) variation of galloping vs. Y. Solid line: stable, dashed line: unstable, $u_1 = 0, u_2 = 0, \nu = 8$.

3. **Applications and Results**

In this section, we analyze the effect of the amplitude Y of the combined excitation on the vibration of the tower for different types of turbulent wind flow. For convenience, the parameter values used in the present study are taken from Luongo and Zulli, (2011a).

3.1 *Case of non-turbulent wind*

The equilibria of Eq. (8), corresponding to periodic oscillations of the system, are giving by setting $\dot{a} = \dot{\phi} = 0$. In the absence of turbulence ($u_1 = u_2 = 0$), only the first equation of system (8) is used. Besides the trivial solution, $a = 0$, the amplitude of the self-excitation is also obtained, such as

$$a = \sqrt{\frac{4(c_a V + H_0 - H_1 b_{31})}{3 b_{31} H_2}} \tag{9}$$

Figure 1a shows the galloping amplitude a versus the wind velocity V in the absence of the unsteady wind ($u_1 = 0, u_2 = 0$), as given by Eq. (9), for $\sigma = 0$ and for different values of the amplitude Y of the combined excitation. The trivial solution exists everywhere and changes its stability at the bifurcation point. It can be seen from this figure that increasing the amplitude Y, the amplitude of the galloping decreases significantly and the location of the galloping onset shifts toward higher values of the steady wind velocity. The variation of the galloping amplitude versus the amplitude of the FHE and the IPD, Y, is reported in Fig. 1b showing the decrease of the amplitude for different values of the steady wind velocity V, as Y is increased. For comparison with Fig. 1a, we show in Fig. 2a the effect of IPD on galloping indicating a decrease in the amplitude only, while 2b depicts the effect of external excitation on galloping showing a shift of the galloping onset only.

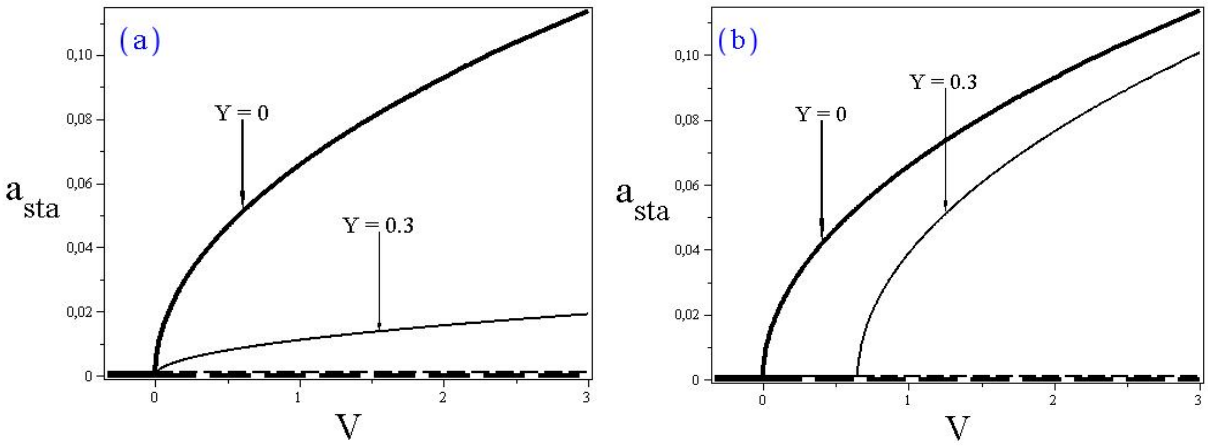

Figure 2. (a) Effect of IPD only on galloping vs. V, (b) effect of external excitation only. Solid line: stable, dashed line: unstable, $u_1 = 0$, $u_2 = 0$, $\nu = 8$.

3.2 *Case of turbulent wind with external excitation*

In the case of turbulent wind with external excitation ($u_1 \neq 0, u_2 = 0$), analysis of equilibria of the slow flow (8) yields the following amplitude-response equation

$$\frac{(S_1 a - S_2 a^3)^2}{(\beta + S_5 a^2)^2} + \frac{(-\sigma a)^2}{(\beta + 3S_5 a^2)^2} = 1 \tag{10}$$

In this case, the variation of the galloping versus the wind velocity V, as given by Eq. (10), is shown in Fig. 3a for a given value of the external excitation u_1. The solid line corresponds to the stable branch, the dashed line corresponds to the unstable one and circles are obtained by numerical simulation. One observes, as in the previous case of excitation, that the combined effect of the FHE and the IPD decreases significantly the galloping amplitude and shifts substantially the frequency response torward higher values of wind velocity. For comparison, Fig. 4 (picked from Belhaq et al, 2013a; Mokni et al, 2014) depicts, respectively, the effect of external excitation (Fig. 4a) and the internal parametric damping (Fig. 4b) on the galloping. The variation of the galloping amplitude versus the amplitude Y is illustrated in Fig. 3b for different values of wind velocity showing a decreasing of the galloping amplitude for increasing Y.

Figure 5a shows the effect of the amplitude Y on the galloping versus σ indicating effectively that the galloping amplitude decreases with increasing Y. The variation of the galloping versus Y is shown in Fig. 5b for two different values of the detuning. The effect of external excitation and the IPD are also reported in Fig. 6 (picked from Belhaq et al, 2013a; Mokni et al, 2014) for comparison, showing a decreasing of the galloping amplitude.

3.3 *Case where turbulent wind activates parametric excitation*

In the case of turbulent wind with parametric excitation ($u_1 = 0, u_2 \neq 0$), the corresponding amplitude response equation is written as

$$\frac{(-S_1 a + S_2 a^3)^2}{(-S_3 a + 2S_4 a^3)^2} + \frac{(-\sigma a)^2}{(-S_3 a + S_4 a^3)^2} = 1 \tag{11}$$

Figure 7a shows, for a given value of the excitation u_2, the effect of the amplitude Y of the FHE and the IPD on the galloping versus V, as given by (11), indicating a decrease and a shift to the right in the frequency response of

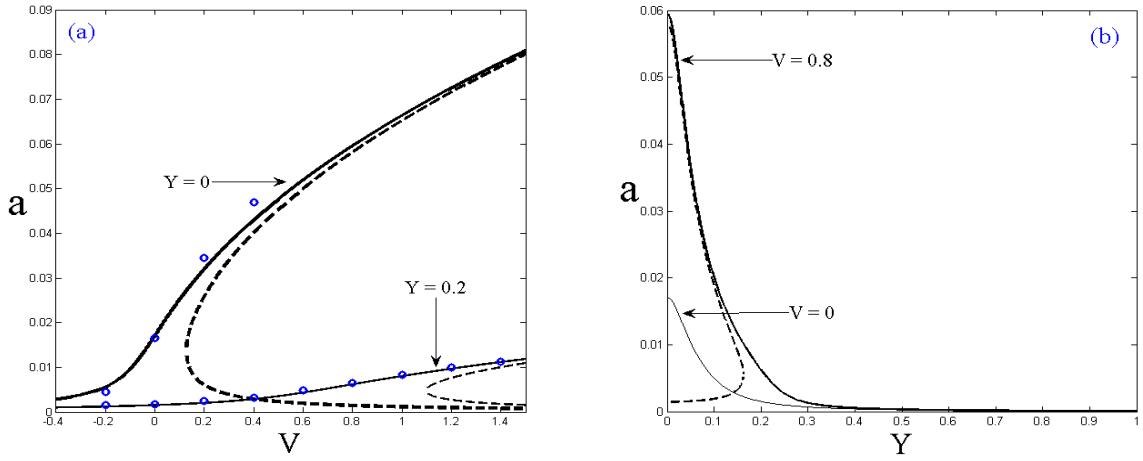

Figure 3. (a) Effect of combined FHE and IPD on the galloping amplitude vs. V, (b) variation of galloping vs. Y, $u_1 = 0.1$, $\sigma = 0$, $\nu = 10$. Solid line: stable; dashed line: unstable; circle: numerical simulation.

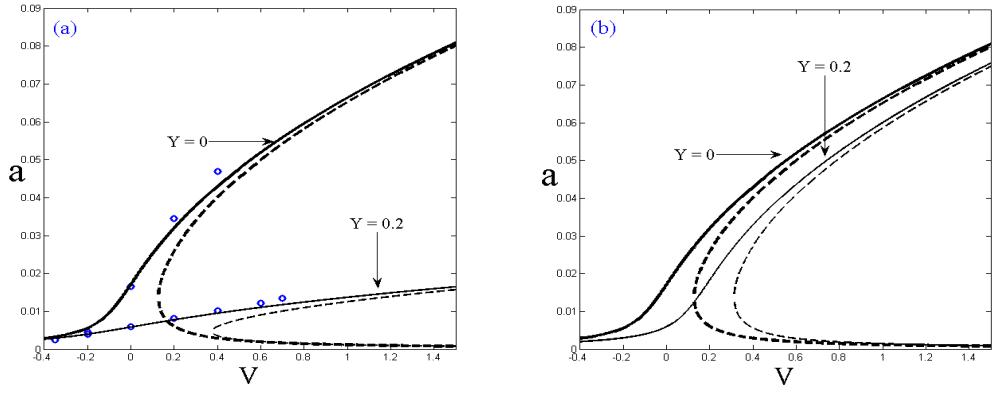

Figure 4. (a) Effect of IPD on the galloping vs. V; $u_1 = 0.1$, $\sigma = 0$, $\nu = 10$, (b) effect of external excitation for the same values of parameters. (picked from Belhaq et al, 2013a; Mokni et al, 2014); Solid line: stable; dashed line: unstable; circle: numerical simulation.

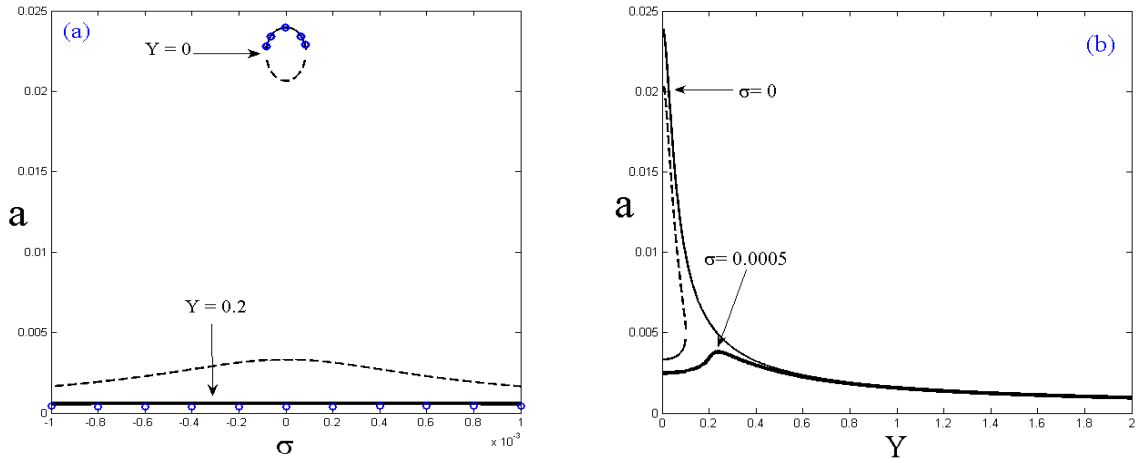

Figure 5. (a) Effect of FHE and IPD on the galloping amplitude vs. V, (b) variation of galloping vs. Y, $u_1 = 0.1$, $\sigma = 0$, $\nu = 10$. Solid line: stable; dashed line: unstable; circle: numerical simulation.

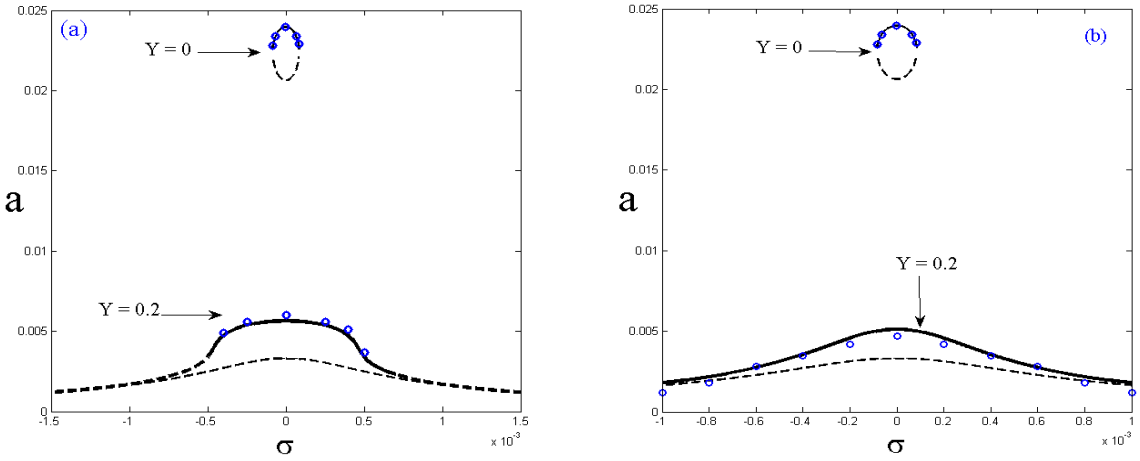

Figure 6. (a) Effect of the IPD on the galloping vs. σ, (b) effect of external excitation (picked from Belhaq et al, 2013a; Mokni et al, 2014). Solid line: stable; dashed line: unstable; circle: numerical simulation; $u_1 = 0.033$, $\nu = 10$, $V = 0.117$.

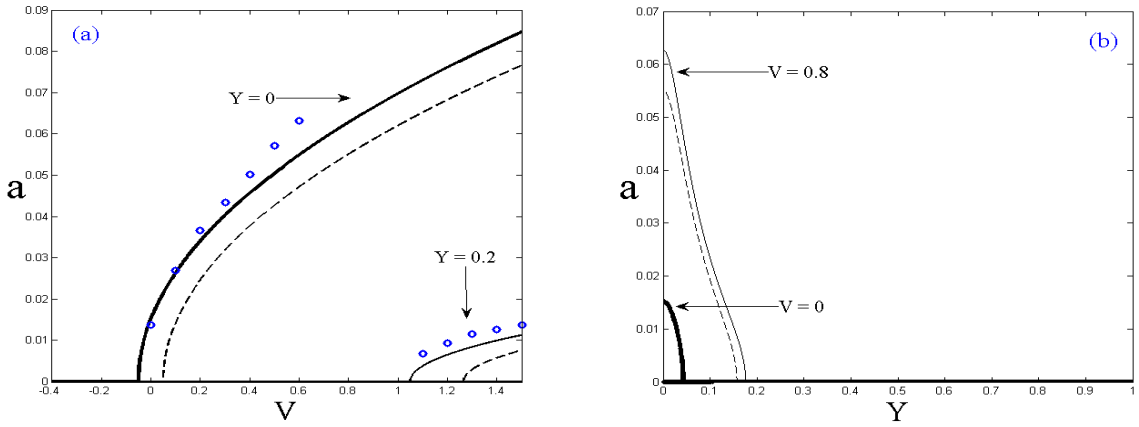

Figure 7. (a) Effect of Y on galloping; $u_2 = 0.1$, $\sigma = 0$, $\nu = 8$, (b) variation of galloping vs. Y. Solid line: stable; dashed line: unstable; circle: numerical simulation.

the galloping amplitude Y is increased. The variation of the galloping versus Y is shown in Fig. 7b for different values of the steady wind velocity. Figure 8 a,b (picked from Belhaq et al, 2013a; Mokni et al, 2014) depicts, respectively, the effect of external excitation and IPD on the galloping onset, for comparison.

The effect of the amplitude of the FHE and the IPD on the galloping amplitude versus σ is shown in Fig. 9a. A substantial decrease of the galloping amplitude by increasing Y is depicted. Figure 9b,c (picked from Belhaq et al, 2013a; Mokni et al, 2014) illustrates, respectively, the effect of IPD and external excitation for comparison.

3.4 *Case where turbulent wind activates external and parametric excitations*

In the case where the external and parametric excitations are both present $(u_1 \neq 0, u_2 \neq 0)$, the amplitude-frequency response is shown in Fig. 10. The plots indicate the effect the amplitude Y on the frequency response showing that increasing Y eliminates the bistability in the amplitude response, thereby the coexistence of two different amplitudes of oscillation. Figure 10b,c picked from (Belhaq et al, 2013a; Mokni et al, 2014) illustrates, respectively, the effect of the IPD and external excitation for comparison.

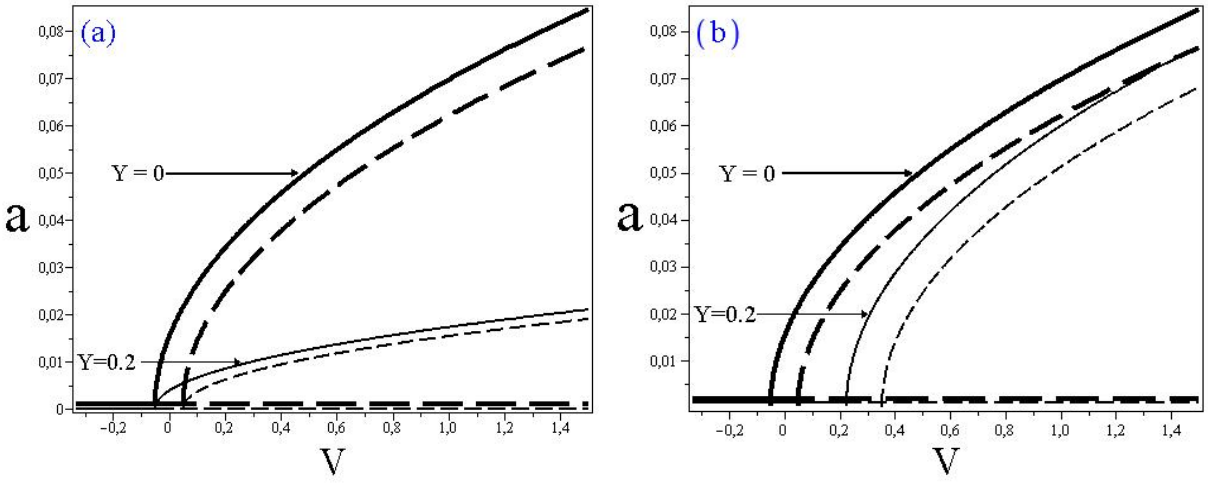

Figure 8. (a) Effect of IPD on galloping vs. V, (b) effect of external excitation (picked from Belhaq et al, 2013a; Mokni et al, 2014). Solid line: stable; dashed line: unstable; circle: numerical simulation; $u_2 = 0.1, \sigma = 0, \nu = 8$.

4. Conclusion

In this work, we have investigated the effect of FHE and IPD on the amplitude and the onset of periodic galloping of a tower when submitted to steady and turbulent wind flow. A lumped mass sdof model was considered and attention was focused on the case where the turbulent wind activates either external excitation, parametric one or both. The method of DPM and the MSM are used to drive a slow dynamic near primary resonance. It is shown that in the case of steady wind, the combined effect of FHE and IPD retards substantially the galloping onset and decreases significantly its amplitude. The results also shown that in the case of turbulent wind, the FHE and IPD also decreases the amplitude of the galloping and increases the galloping onset of the tower in all cases of turbulent wind.

Appendix I

The expression of the coefficients of Eq. (1) are:

$$\omega = \pi\frac{\sqrt{3EI}}{h\ell\sqrt{m}},\quad c_a = \frac{\rho A_1 bh\ell\bar{U}_c}{2\pi\sqrt{3EIm}},\quad b_1 = c_a,\quad b_2 = -\frac{4\rho A_2 b\ell}{3\pi m},\quad b_{31} = -\frac{3\pi\rho A_3 b\ell\sqrt{3EI}}{8h\bar{U}_c\sqrt{m^3}}$$

$$b_{32} = -b_{31},\quad \eta_1 = \frac{4\rho A_0 bh^2\ell\bar{U}_c^2}{3\pi^3 EI},\quad \eta_2 = \frac{\eta_1}{2},\quad U(t) = \bar{U} + u(t),$$

where ℓ is the height of the tower, b the cross-section wide, EI the total stiffness of the single story, m the mass longitudinal density, h the inter story height, and ρ the air mass density. $A_i, i = 0,...3$ are the aerodynamic coefficients for the squared cross-section. The dimensional critical velocity is given by

$$\bar{U}_c = \frac{4\pi\xi\sqrt{3EIm}}{\rho b A_1 h\ell}$$

where ξ is the modal damping ratio, depending on both the external and internal damping according to

$$\xi = \frac{\zeta h^2}{24EI}\omega + \frac{c_0}{2m\omega}$$

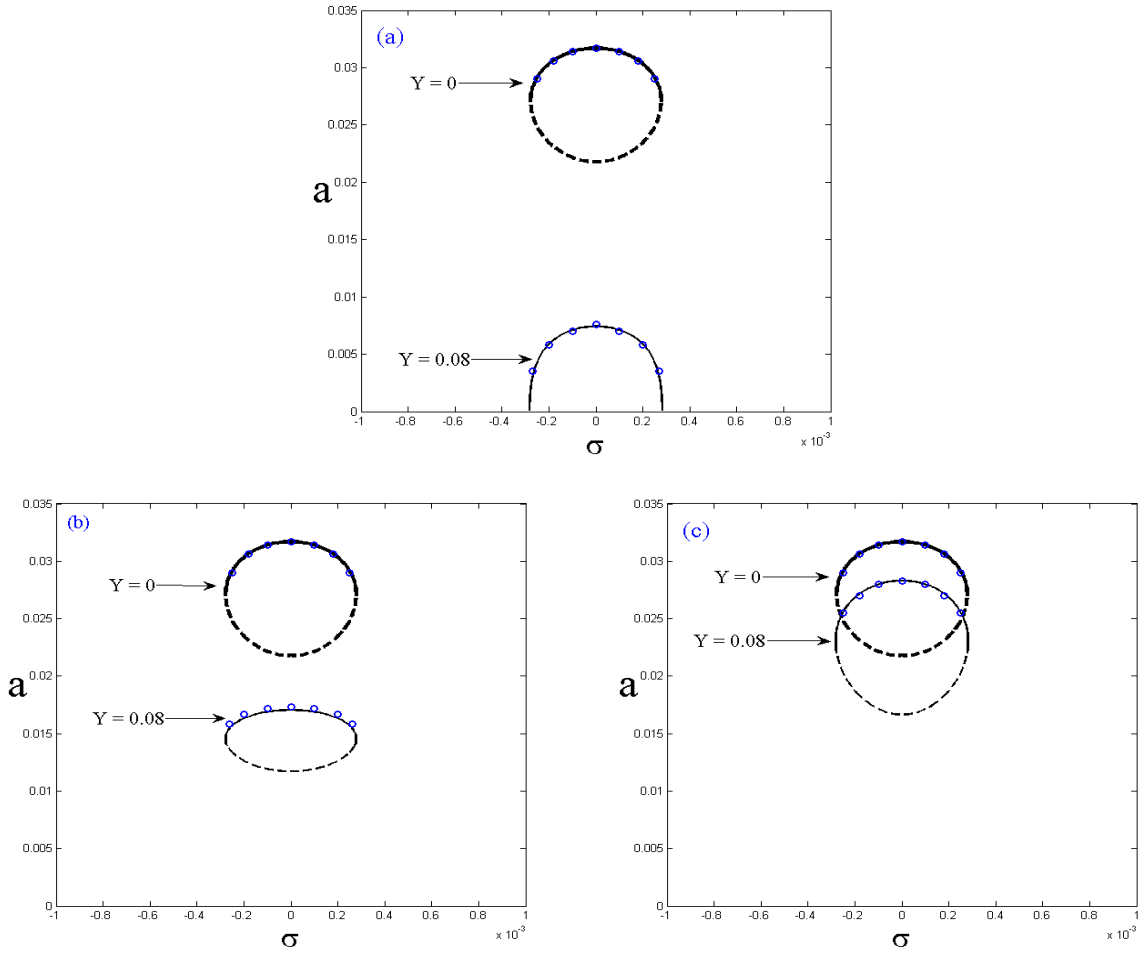

Figure 9. (a) Effect of Y of the FHE and the IPD on galloping, (b) effect of IPD on galloping vs. V, (c) effect of external excitation (picked from Belhaq et al, 2013a; Mokni et al, 2014), $u_2 = 0.1$, $V = 0.167$, $\nu = 8$. Solid line: stable; dashed line: unstable; circle: numerical simulation.

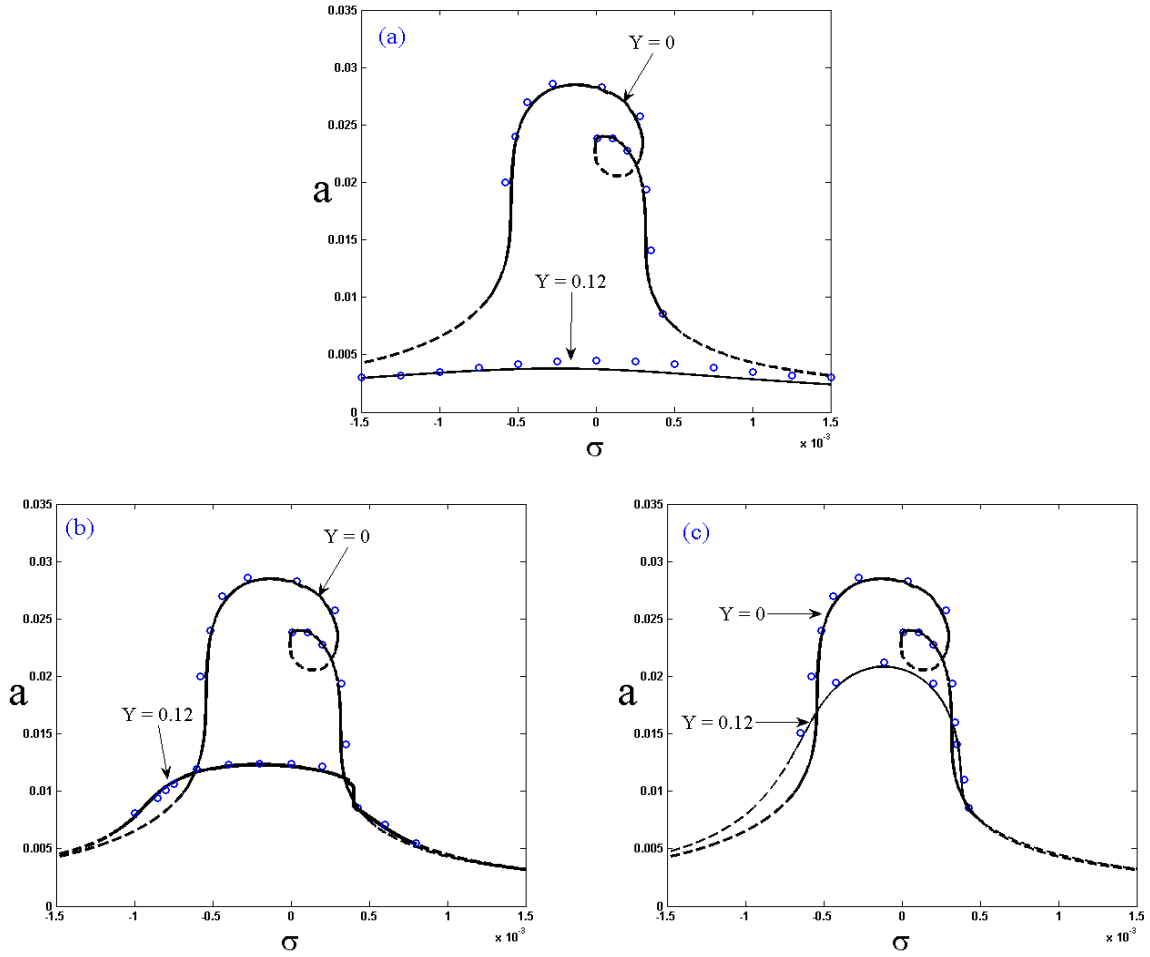

Figure 10. (a) Effect of Y of the FHE and the IPD on galloping,(b) effect of IPD and (c) effect of external excitation (picked from Belhaq et al, 2013a; Mokni et al, 2014) for $V = 0.11$, $u_1 = 0.1$, $u_2 = 0.1$. Solid line: stable, dashed line: unstable, circle: numerical simulation.

where ζ and c_0 are the external and internal damping coefficients, respectively. Introducing a parametric damper device in the internal damping such as

$$c_0 = c(1 + y_0\nu^2 \cos \nu t)$$

where y_0 and ν are the amplitude and the frequency of the internal PD, respectively. In this case the equation of motion reads

$$\ddot{x} + x + \big[c_a + Y\nu^2 \cos \nu t\big]\dot{x} - c_a\big[\bar{U} + u(t)\big]\dot{x} + b_2\dot{x}^2 + \big[\frac{b_{31}}{\bar{U}} + \frac{b_{32}}{\bar{U}^2}u(t)\big]\dot{x}^3 = \eta_1\bar{U}u(t) + \eta_2\bar{U} + Y\cos(\nu t) \tag{12}$$

where $Y = \frac{cy_0}{m\omega}$. Re-arranging terms yields the equation of motion (1).

Appendix II

Introducing $D_i^j \equiv \frac{\partial^j}{\partial^j T_i}$ yields $\frac{d}{dt} = \nu D_0 + D_1$, $\frac{d^2}{dt^2} = \nu^2 D_0^2 + 2\nu D_0 D_1 + D_1^2$ and substituting Eq. (2) into Eq. (1) gives

$$\begin{aligned}\mu^{-1}D_0^2\phi + D_1^2 z + 2D_0D_1\phi + \mu D_1^2\phi + \big(c_a(1-\bar{U}) - b_1u(t)\big)\big(D_1z + D_0\phi + \mu D_1\phi\big) + z \\ +\mu\phi + Y\nu^2\cos(\nu t)\big(D_1z + D_0\phi + \mu D_1\phi\big) + b_2\big((D_1z)^2 + 2D_1z(D_0\phi + \mu D_1\phi) + (D_0\phi)^2 \\ +2\mu D_0\phi D_1\phi + (\mu D_1\phi)^2\big) + \big(\frac{b_{31}}{\bar{U}} + \frac{b_{32}}{\bar{U}^2}u(t)\big)\big((D_1z)^3 + 3(D_1z)^2(D_0\phi \\ +\mu D_1\phi) + 3(D_1z)(D_0\phi + \mu D_1\phi)^2 + (D_0\phi + \mu D_1\phi)^3\big) = \eta_1\bar{U}u(t) + \eta_2\bar{U}^2 + Y\cos(\nu t)\end{aligned} \tag{13}$$

Averaging (13) leads to

$$\begin{aligned}D_1^2 z + \big(c_a(1-\bar{U}) - b_1u(t)\big)D_1z + z + Y\nu^2 < \cos(T_0)\big(D_0\phi + \mu D_1\phi\big) > + b_2\big((D_1z)^2 \\ + < (D_0\phi)^2 > + < (2\mu D_0\phi D_1\phi) > + < (\mu D_1\phi)^2 > \big) + \big(\frac{b_{31}}{\bar{U}} + \frac{b_{32}}{\bar{U}^2}u(t)\big)\big((D_1z)^3 \\ +3D_1z(< (D_0\phi)^2 > + < (2\mu D_0\phi D_1\phi) > + < (\mu D_1\phi)^2 >)\big) = \eta_1\bar{U}u(t) + \eta_2\bar{U}^2\end{aligned} \tag{14}$$

Subtracting (14) from (13) yields

$$\begin{aligned}\mu^{-1}D_0^2\phi + 2D_0D_1\phi + \mu D_1^2\phi + \big(c_a(1-\bar{U}) - b_1u(t)\big)\big(D_0\phi + \mu D_1\phi\big) + \mu\phi + Y\nu^2\cos(T_0)\big(D_0\phi \\ +\mu D_1\phi\big) - Y\nu^2 < \cos(T_0)\big(D_0\phi + \mu D_1\phi\big) > + b_2\big(2D_1z(D_0\phi + \mu D_1\phi) + (D_0\phi)^2 - < (D_0\phi)^2 > \\ +2\mu D_0\phi D_1\phi - < 2\mu D_0\phi D_1\phi > + (\mu D_1\phi)^2 - < (\mu D_1\phi)^2 > \big) + \big(\frac{b_{31}}{\bar{U}} + \frac{b_{32}}{\bar{U}^2}u(t)\big)\big(3(D_1z)^2(D_0\phi \\ +\mu D_1\phi) + 3D_1z(D_0\phi)^2 - 3D_1z < (D_0\phi)^2 > + 6D_1z\mu(D_0\phi D_1\phi) - < 6D_1z\mu(D_0\phi D_1\phi) > \\ +3D_1z(\mu D_1\phi)^2 - 3D_1z < (\mu D_1\phi)^2 > + (D_0\phi)^3 + 3\mu(D_0\phi)^2 D_1\phi + 3D_0\phi(\mu D_1\phi)^2 \\ +(\mu D_1\phi)^3\big) = Y\cos(\nu t) - Y\nu^2\cos(T_0)D_1z\end{aligned} \tag{15}$$

Using the inertial approximation (Blekhman, 2000), i.e. all terms in the left-hand side of Eq. (15), except the first, are ignored, one obtains

$$\phi = (Y\nu(D_1z) - \frac{Y}{\nu})\cos(T_0) \tag{16}$$

Inserting ϕ from Eq. (16) into Eq. (14), using that $< cos^2 T_0 >= 1/2$, and keeping only terms of orders three in z, give the equation governing the slow dynamic of the motion (3).

References

[1] Parkinson, G.V., Smith, J.D., 1964. The square prism as an aeroelastic non-linear oscillator, Quarterly Journal of Mechanics and Applied Mathematics 17, 225-239.

[2] Novak, M., 1969. Aeroelastic galloping of prismatic bodies, ASCE, Journal of Engineering Mechanics Division 96, 115-142.

[3] Nayfeh, A.H., Abdel-Rohman, M., 1990a. Galloping of squared cantilever beams by the method of multiple scales, Journal of Sound and Vibration 143, 87-93.

[4] Abdel-Rohman, M., 2001b. Effect of unsteady wind flow on galloping of tall prismatic structures, Nonlinear Dynamics 26, 231-252.

[5] Clark, R., Modern, A., 2004. Course in Aeroelasticity, fourth ed, Kluwer Academic Publishers, Dordrecht, The Netherlands.

[6] Spencer Jr, B.F., Nagarajaiah, S., 2003. State of the art of structural control, Journal of Structural Engineering 129, 845-865.

[7] Nayfeh, A.H., Balachandran, B., 1995. Applied Nonlinear Dynamics, John Wiley, New York.

[8] Luongo, A., Zulli, D., 2011a. Parametric, external and self-excitation of a tower under turbulent wind flow, Journal of Sound and Vibration 330, 3057-3069.

[9] Zulli, D., Luongo, A., 2012b. Bifurcation and stability of a two-tower system under wind-induced parametric, external and self-excitation, Journal of Sound and Vibration 331, 365-383.

[10] Belhaq, M., Kirrou, I., Mokni, L., 2013a. Periodic and quasiperiodic galloping of a wind-excited tower under external excitation, Nonlinear Dynamics 74, 849-867.

[11] Keightley, W.O., Housner, G.W., Hudson, D.E., 1961. Vibration tests of the Encino dam intake tower, California Institute of Technology, Report No. 2163, Pasadena, California.

[12] Mokni, L., Kirrou, I., Belhaq, M., 2014. Galloping of a wind-excited tower under internal parametric damping, Journal of Vibration and Acoustics doi: 10.1115/1.4026505.

[13] Munteanu, L., Chiroiu, V., Sireteanu, T., 2013. On the response of small buildings to vibrations, Nonlinear Dynamics 73, 1527-1543.

[14] Blekhman, I.I., 2000. Vibrational Mechanics, Nonlinear Dynamic Effects, General Approach, Applications, Singapore: World Scientific.

[15] Thomsen, J.J., 2003. Vibrations and Stability: Advanced Theory, Analysis, and Tools, Springer- Verlag, Berlin-Heidelberg.

[16] Lakrad, F., Belhaq, M., 2010. Suppression of pull-in instability in MEMS using a high-frequency actuation, Communication in Nonlinear Science and Numerical Simulation 15, 3640-3646.

[17] Kirrou, I., Mokni, L., Belhaq, M., 2013b. On the quasiperiodic galloping of a wind-excited tower, Journal of Sound and Vibration 332, 4059-4066.